A NEW 2-D GaAs MESFETs MODEL BASED ON A VERY ACCURATE VELOCITY - FIELD EXPRESSION

B. M. Bobbo, A. Giorgio, V. M. N. Passaro, A. G. Perri, M. Pesare

Dipartimento di Elettrotecnica ed Elettronica, Politecnico di Bari
Via E. Orabona 4, 70125 Bari, Italy
Phone: + 39 – 80 – 5460427 / 5460314 Fax: + 39 – 80 – 5460410 E-Mail: perri@poliba.it

Abstract – **A new physical model for GaAs MESFET drain current and gate capacitance based on the Chang-Fetterman velocity–electric field model, is presented. Accurate analytical expressions for the 2-D channel potential in the saturation region are adequately employed and mathematically manipulated in order to develop a 2-D C-V physical MESFET model without the main approximations used up to now in the previous physical models.**

I. INTRODUCTION

Physical I-V models of GaAs MESFETs represent an important CAD tool to obtain detailed previsions of the transistor behavior as a function of geometrical and physical parameters, i.e. technological factors.

In particular, this allows the designer to predict the performance of epitaxial or implanted FETs, and self-aligned or not self-aligned gate FETs.

Moreover, a full consistent and accurate I-V physical model can be regarded as the first step to develop a physical C-V model, by calculating the electron charges from current data and deriving with respect to the applied voltages.

However, the physical models already presented in literature [1-5] cannot generally be used to predict any experimental and technological condition, and different approaches are typically used. The main differences between these approaches concern the numerical solution technique (Green function, variable separation, etc.), the second order effects involved (backgating effect, high field effects, surface states) and the mathematical expression of the velocity – electric field dependence assumed.

In this paper, the Chang-Fetterman velocity-electric field function is assumed, since it represents the best approximation with respect to experimental and numerical data (e.g. Monte Carlo method [1]).

In Section II, a brief explanation of the model, which is derived from the approach presented in [2], is given. In Section III the Chang-Fetterman model is used to derive a physical model for MESFET C-V characteristics. Section IV presents the numerical results compared with measurements whereas Section V summarizes the contents of this paper.

II. I-V MODEL

The proposed model is based on the following relation between the electric field E and the charge drift velocity v [2]:

$$v = \frac{\mu \cdot E}{\sqrt{1+\left(\frac{E-E_L}{E_C}\right)^2 \cdot u(E-E_L)}} \qquad (1)$$

where $u(E-E_L)$ is the step function, $E_C = v_S/\mu$ is the critical field, v_S is the saturation velocity, μ is the low-field mobility, E_L is defined as follows:

$$E_L = \frac{1}{2}\left(E_T + \sqrt{E_T^2 - 4E_C^2}\right) \qquad (2)$$

and E_T is the electric field value corresponding to the velocity peak.

At low drain voltage, Eq. (1) is a linear relation between velocity and electric field, i.e. $v = \mu \cdot E$. In this case, a simple 1-D Poisson equation is to be solved:

$$\frac{\partial^2 V}{\partial y^2} = -\frac{qN_D(y)}{\varepsilon_S} \qquad (3)$$

in which ε_S is the GaAs dielectric permittivity, q is the elementary charge and $N_D(y)$ is an arbitrary doping concentration profile. After a double integration, the solution of Eq. (3) is:

$$V(x,y) = -\frac{q}{\varepsilon_S}\int_0^y\left(\int_0^y N_D(y)dy\right)dy + V_0 + \frac{q\cdot y}{\varepsilon_S}\int_0^{h(x)} N_D(y)dy \qquad (4)$$

in which $V_0 = V_{GS} - V_{bi}$, V_{GS} is the gate-source voltage, V_{bi} is the built-in voltage and h(x) is the spatial charge region profile, depending on the abscissa x along the channel. The channel current-continuity equation is given by:

$$I_C = qZ\frac{dV}{dx}\int_{h(x)}^{a} N_D(y)\mu(y)dy \qquad (5)$$

in which Z is the gate width and a is the channel thickness. Combining Eqs. (4) and (5), the current-voltage relation can be expressed as:

$$I_C = \frac{q^2 Z}{\varepsilon_S L}\int_{h_0}^{h_L} h\cdot N_D(h)\left(\int_h^a N_D(y)\mu(y)dy\right)dh \qquad (6)$$

in which $h_0 = h(x=0)$ and $h_L = h(x=L)$, L being the gate

length; furthermore, h_0 and h_L are obtained by imposing the following boundary conditions:

$$V(h_0) = V_S + I_C \cdot R_S \quad (7)$$

$$V(h_L) = V_D + I_C \cdot R_D \quad (8)$$

where R_S and R_D are the source-to-channel and drain-to-channel resistance, respectively. In the linear region, the electric field is always less than E_L, thus the maximum depletion width in this region, said h_a, is less than h_L.

When the drain-source voltage increases, the electric field becomes larger than E_L, thus beneath the gate two regions can be distinguished, one for $0<x<L_a$ ($E<E_L$) and the other for $L_a<x<L$ ($E_L<E<E_T$).

Substituting Eq. (1) in Eq. (5):

$$I_C = qZ \frac{E}{\sqrt{1+\left(\frac{E-E_L}{E_C}\right)^2}} \int_h^a N_D(y)\mu(y)dy \quad (9)$$

Since $E = dV/dx$ and $E<E_T$, it is possible to write:

$$dV \cdot \frac{1+\sqrt{(1+c^2)\beta^2 - c^2}}{E_L(1+c^2)} = dx \quad (10)$$

in which $c = E_C/E_L$ and

$$\beta = \frac{qZE_C \int_h^a N_D(y)\mu(y)dy}{I_C}$$

Using the expression derived by (3) leads to:

$$dV = \frac{dV}{dh} \cdot dh = \frac{qN_D(h)h}{\varepsilon_S} dh \quad (11)$$

combining (10) and (11) and integrating between L_a and L, the current-voltage law in the knee region is obtained:

$$L - L_a = \frac{q}{\varepsilon_S E_L (1+c^2)} \int_{h_a}^{h_b} N_D(h)h\left(1+\sqrt{(1+c^2)\beta^2 - c^2}\right)$$

$$L_a = \frac{q^2 Z}{\varepsilon_S I_C} \int_{h_0}^{h_a} hN_D(h)\left(\int_h^a N_D(y)\mu(y)dy\right)dh$$

which is valid if $E< E_T$.

For $E> E_T$, when the drain-source voltage further increases, the device operates in the high field saturation region.

In the saturation region the usual gradual channel approximation becomes poor. Then, the 2-D Poisson equation has to be solved. The channel beneath the gate can be divided into three regions, for $0<x<L_a$ ($E<E_L$), $L_a<x<L_b$ ($E_L<E<E_T$) and $L_b<x<L$ ($E>E_T$). The current-voltage characteristic is obtained by imposing:

$$L = L_a + L_b + L_2 \quad (12)$$

in which L_2 is the channel region extension where $E > E_T$ and L_b is obtained from the subsequent equation with h_T instead of h_L:

$$L_b = \frac{q}{\varepsilon_S E_L (1+c^2)} \int_{h_a}^{h_T} N_D(h)h\left(1+\sqrt{(1+c^2)\beta^2 - c^2}\right)dh$$

The unknown variable L_2 is obtained by solving the following system of two non-linear equations:

$$L_3^2 = h_T^2 \cdot E_T \frac{\exp\left(\frac{\pi L_2}{2h_T}\right) - 1 - \sinh\left(\frac{\pi L_2}{2h_T}\right) \cdot \exp\left(-\frac{\pi L_3}{2h_T}\right)}{E_D - E_T \cdot \cosh\left(\frac{\pi L_2}{2h_T}\right) + E_{FC}} \quad (13)$$

$$V(L_3) - V(-L_2) = \frac{1}{3}E_T L_3\left(1+2\exp\left(\frac{\pi L_2}{2h_T}\right)\right) + E_T \sinh\left(\frac{\pi L_2}{2h_T}\right) \cdot \exp\left(-\frac{\pi L_3}{2h_T}\right)\left(\frac{2h_T}{\pi} + \frac{L_3}{3}\right) \quad (14)$$

with: $V(L_3) = V_{DS} - I_C R_D$, $E_D = \frac{q}{\varepsilon_s}\int_0^{h_T} N_D(y)dy$

and $V(-L_2) = V(h_T)\big|_{x=-L_2}$ having used Eq. (4). L_3 is the maximum extension of the saturation depletion region out of the gate, where a constant width h_T has been assumed. E_{FC} is the surface field due to the fixed charge in the passivation insulator. Eqs. (13) and (14) are obtained by solving the 2-D Poisson equation in the saturation region. Details of the analytical procedure can be found in [2].

III. C-V MODEL

Extending the physical model presented above, it is possible to define a set of relations in order to calculate the MESFET C-V characteristics. The analyzed capacitance are the C_{gs} and C_{gd}, defined below:

$$C_{gd} = \frac{\partial Q}{\partial V_d}, \quad V_g = \text{cost}, \; V_s = \text{cost},$$

$$C_{gs} = \frac{\partial Q}{\partial V_s}, \quad V_g = \text{cost}, \; V_s = \text{cost}$$

Q being the charge in the depletion region in the active channel of the device.

The main contribution to Q is the charge beneath the gate, defined as follows:

$$Q_g = qZ\int_0^L\left[\int_0^{h(x)} N_D(y)dy\right]dx$$

in which q is the electron charge, Z the gate width, L the gate length, $N_D(y)$ the doping profile, but for the sake of accuracy it must be considered also the charge in the depletion region extended out of the gate. The gate charge evaluation is quite simple, if the spatial charge region profile is known.

The main difference between the previous technique to determine the extent of the depletion region and the proposed analytical method is that approximates relations deriving from numerical bi-dimensional simulations [6,7] are replaced by a 2-D more accurate analytical closed-form solution of the Poisson equation with a more accurate

v-E relation.

The operating condition in which the model is developed is the saturation condition. To this aim in the following sections the three main regions are distinguished and, for each one, the necessary relations to evaluate the gate charge are given. Once the gate charge Q_g has been calculated, it is possible to obtain the required capacitance executing simple derivatives

A. Linear Region

In the linear region the channel current as follows:

$$I_C = qZE_X G(h) \tag{15}$$

in which:

$$G(h) = \int_{h(x)}^{a} N_D(y)\mu(y)dy$$

where E_x is the electric field in the channel, calculated at the abscissa x. To evaluate E_x it is sufficient to execute the derivative of the voltage with respect to x; the voltage and the electric field are reported below:

$$V(x) = -\frac{q}{\varepsilon_S}\cdot\int_0^{h(x)}\left[\int_0^{h(\beta)} N_D(\alpha)\cdot d\alpha\right]\cdot d\beta + V_0 + \frac{q\cdot h(x)}{\varepsilon_S}\cdot\int_0^{h(x)} N(\alpha)\cdot d\alpha$$

$$E_x = \frac{\partial V(x)}{\partial x} = \frac{\partial V(h)}{\partial h}\cdot\frac{\partial h(x)}{\partial x} = f(h)\cdot\frac{dh(x)}{dx}$$

in which:

$$f(h) = \frac{qhN_D(h)}{\varepsilon_S}$$

by substituting the previous electric field expression in (15), I_C is expressed as:

$$I_C = qZ\cdot f(h)\frac{dh(x)}{dx}G(h)$$

Thus, the differential equation can be solved by separating the variables and integrating:

$$\frac{I_C}{qZ}\int_0^x dx = \int_0^h f(h)G(h)dh$$

Once the bias condition and the abscissa x are fixed, Q_g can be calculated first evaluating h(x) and then integrating according to the definition. For example in the case of uniform doping the non-linear equation is:

$$\frac{h^3}{3} - \frac{a\cdot h^2}{2} + \frac{a\cdot h_0^2}{2} - \frac{h_0^3}{3} + \frac{I_C\cdot x\cdot\varepsilon_S}{N_D^2\cdot q^2\cdot Z\cdot\mu} = 0$$

the solution of which leads to the spatial charge profile.

B. Knee Region

In the knee region the channel current can be expressed as follows:

$$I_C = \frac{qZE_x}{\sqrt{1+\left(\frac{E_x - E_L}{E_C}\right)^2}}G(h) \tag{16}$$

After easy mathematical manipulations it can be written as:

$$E_x = \frac{E_L(1+c^2)}{1+\sqrt{1+(1+c^2)\beta^2 - c^2}}$$

being:

$$c = \frac{E_C}{E_L}$$

$$\beta = \frac{qZE_C}{I_C}G(h)$$

Recalling the electric field expression and substituting it in the (16), the following equation is obtained:

$$f(h)\cdot\frac{d(h(x))}{d(x)} = \frac{E_L\cdot\left(1+c^2\right)}{1+\sqrt{\left(1+c^2\right)\cdot\beta^2 - c^2}}$$

Also in this case, the differential equation can be solved by separating the variables and integrating:

$$E_L\cdot\left(1+c^2\right)\cdot\int_{L_a}^{x} dx = \int_{h_a}^{h} f(h)\cdot\left[1+\sqrt{\left(1+c^2\right)\cdot\beta^2 - c^2}\right]\cdot dh$$

In correspondence of each arbitrary bias conditions and abscissa x, h(x) can be evaluated by solving the previous non-linear equation, and Q_g can be evaluated by integrating. For example in the case of uniform doping the relations become:

$$J_1 + J_2 - E_L\cdot\left(1+c^2\right)\cdot(x - L_a) = 0$$

being:

$$J_1 = \frac{q\cdot N_D}{2\cdot\varepsilon_S}\cdot\left(h^2 - h_a^2\right)$$

$$J_2 = \int_{h_a}^{h}\frac{q\cdot N_D\cdot h}{\varepsilon_S}\cdot\sqrt{\left(1+c^2\right)\cdot\left(\frac{q\cdot Z\cdot E_C\cdot N_D\cdot\mu}{I_C}\right)^2\cdot(a-h)^2 - c^2}\cdot dh$$

by solving the previous non linear equation, h(x) can be calculated, being x in the range determined by L_a and L_b. The relations about the range $[0,L_a]$ are detailed in the foregoing section.

C. Saturation Region

In this case it is not necessary to solve non-linear equations to evaluate the gate charge, as in the saturation region, when x is varying between L_a and $L_b + L_a$, the spatial charge region has a nearly constant profile, which is fixed at the value h_t, calculated during the solution of the device bias problem. It is sufficient to use the expression below:

$$Q_{g,sat} = q\cdot Z\cdot\int_{L_a+L_b}^{L_a+L_b+L_2+L_3}\left[\int_0^{h_t} N_D(y)\cdot dy\right]\cdot dx$$

Regarding the ranges $[0,L_a]$ and $[L_a,L_a+L_b]$ the relations described in the foregoing sections are to be used.

D. Depletion extension charge

Regarding the calculus of these two additional charges, it is supposed that the spatial charge region close to the gate is circular, which is a quite common supposition in literature.

Therefore the two charges have the following expressions:

$$Q_0 = q \cdot Z \cdot \int_0^{h_0} \left[\int_0^{h_0(x)} N_D(y) \cdot dy \right] \cdot dx$$

$$Q_L = q \cdot Z \cdot \int_0^{h_L} \left[\int_0^{h_L(x)} N_D(y) \cdot dy \right] \cdot dx$$

in which $h_0(x)$ and $h_L(x)$ are the mathematical expressions for a quarter of circle. Considering the case of uniform doping the expressions are:

$$Q_0 = qZN_D \frac{\pi h_0^2}{4}$$

$$Q_L = qZN_D \frac{\pi h_L^2}{4}$$

In the next Section some numerical examples in which the capacitance C_{gd} and C_{gs} are evaluated by deriving the gate charge calculated in the previous way, are reported.

IV. NUMERICAL RESULTS

The model has been tested comparing the numerical results with experimental measurements on the MESFET 2TX102 made by ALCATEL having the following features:

Gate length L (μm)	0.5
Gate width Z (μm)	1200
Active Layer Depth (μm)	0.17
Saturation Velocity v_{sat} (cm/s)	$7\ 10^6$
Mobility μ (cm/V*s)	3800
Substrate Resistance (KΩ)	5
Doping Concentration ($1/cm^3$)	$1.5\ 10^{17}$
Built in Voltage Vbi (V)	0.8

In Figs. 1 and 2, the modeled and experimental characteristics of the considered MESFET in the saturation region are reported.

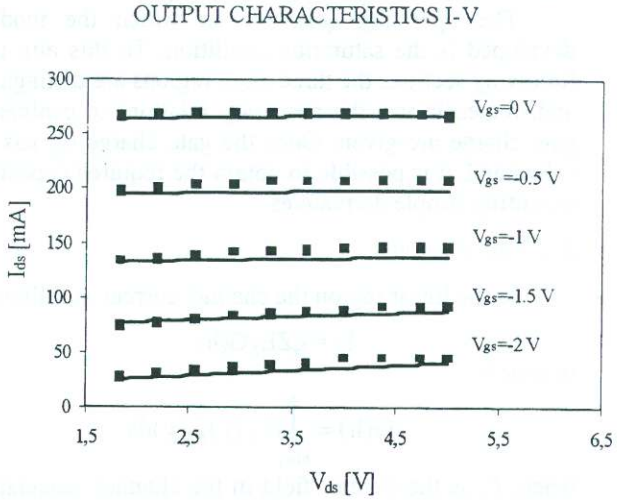

Fig.1: Output characteristics in the saturation region for the considered device: simulated results (solid line) and experimental results '■'.

In Fig. 3 the relative percentage error obtained using both one-dimensional and two-dimensional model is shown.

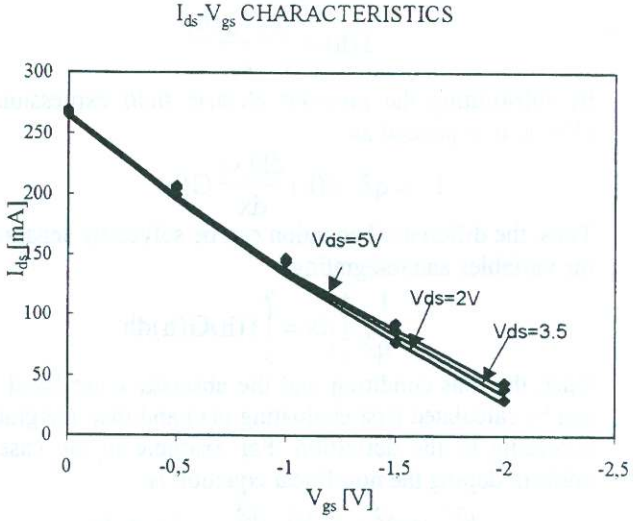

Fig.2: Characteristics I_{ds}-V_{gs} for the considered device: simulated results (solid line) and experimental results '■'.

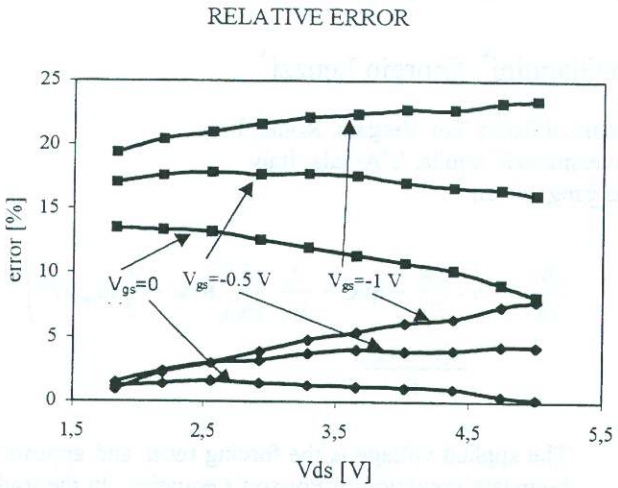

Fig.3: Relative percentage error: one-dimensional model '■' and two-dimensional model '◆'.

The measurements of the capacitance and the comparison with the model results are the present activities in which the authors are engaged. The result that have been presented concern the I-V model and are very promising for further developments both for their accuracy and range of applicability.

V. CONCLUSIONS

In this paper a procedure to improve the approximations that have been used for 20 years up to now to develop a physical 2-D GaAs MESFET model has been proposed.

The most interesting result is the improved calculation of the shape of the depletion region in the FET channel and of the heights and lengths of the three subsections in which it can be divided, starting from an accurate velocity-field model and an analytical solution of the 2-D Poisson equation with the consequent application to determine 2-D I-V and C-V model.

Mathematical difficulties could raise when transforming the channel potential solution into a software implementation; these difficulties have been observed to be strongly application-dependent, i.e. device-dependent. Moreover it has been observed that the main difficulties are related to the exact determination of the parameters included in the velocity-field model.

VI. REFERENCES

[1] R. Anholt," Electrical and Thermal Characterization of MESFETs, HEMTs and HBTs", Artech House, Boston, 1995.

[2] C.-S. Chang and D.-Y. S. Day, "Analytic Theory for Current-Voltage Characteristics and Field Distribution of GaAs MESFET's", *IEEE Trans. on Electron Devices*, vol. **36**, pp. 269-280, 1989.

[3] S.-P. Chin and C.-Y. Wu, "A New I-V Model for Short Gate-Length MESFET's", *IEEE Trans. on Electron Devices*, vol. **40**, pp. 712-720, 1993.

[4] J. Rodriguez-Tellez, K. Mezher, " Improved junction capacitance model for the GaAs MESFET", *IEEE Trans. on Electron Device*, vol.ED-40, pp.2083-2085, 1993.

[5] M. Nawaz, T. Fjeldly, "A new charge conservative capacitance model for GaAs MESFET's", *IEEE Trans. on Electron Device*, vol. ED-44, pp.1813-1821, 1997.

[6] K. Yamaguchi, S. Asai, H. Kodera, "Two-dimensional numerical analysis of stability criteria of GaAs FET's", *IEEE Trans. on Electron Device*, vol. ED-23, pp. 1283-1290, 1976.

[7] K. Yamaguchi, H. Kodera, , "Drain conductance of junction gate FET's in the hot electron range", *IEEE Trans. on Electron Device*, vol. ED-23, pp. 545-553, 1976.